

T. Song
W.-S. Wang
B.-R. Zhou
W.-W. Mai
Z.-Z. Li
H.-C. Guo
F. Zhou

CT and MR Characteristics of Cerebral Sparganosis

BACKGROUND AND PURPOSE: Sparganosis is a rare parasitic infection in humans by a larval cestode of the genus *Spirometra*. Preoperative diagnosis of cerebral sparganosis in the past has been very difficult. Our objective was to evaluate the CT and MR features of cerebral sparganosis in order to make a definite diagnosis.

MATERIALS AND METHODS: We retrospectively reviewed 25 patients (13 male and 12 female; age range, 9–83 years) who proved to have cerebral sparganosis. Fifteen patients underwent MR imaging: 2 patients had CT scanning, and the remaining 8 had both CT and MR scanning. We focused on evaluating the imaging features on CT and MR.

RESULTS: All patients showed edema and degeneration of cerebral white matter. All but 1 had a unilateral lesion. Twenty-two patients had ipsilateral ventricular dilation. The new finding was a tunnel sign, approximately 4 cm in length and 0.8 cm in width, column or fusiform shaped on postcontrast coronal and sagittal MR images ($n = 10$). Thirteen patients showed bead-like enhancement, but solitary ring enhancement was common on the CT images ($n = 2$). The wall of the ring and tunnel appeared isointense or slightly hyperintense on T2-weighted images. Punctate calcifications were seen in 6 patients on CT images but only in 3 patients on the MR images. Hemorrhage was seen in 4 patients on the MR images. An intact whitish, stringlike, living worm was found ($n = 5$).

CONCLUSION: The most characteristic finding was a tunnel sign on postcontrast MR images. The most common finding was bead-shaped enhancement. MR is superior to CT in demonstrating the extent and number of lesions, except punctate calcifications. Combined with clinical data and enzyme-linked immunosorbent assay, the preoperative diagnosis of cerebral sparganosis could be established on MR imaging.

Sparganosis is a rare parasitic infection in humans by a larval cestode of the genus *Spirometra*.^{1,2} It has been believed that humans are considered an accidental intermediate host of *Spirometra mansoni*.¹⁻³ To our knowledge, infection in humans occurs mainly by the ingestion of raw or inadequately cooked flesh of the infected host such as frogs, snakes, and chickens. Other routes of infection include drinking contaminated water or applying the flesh of an infected host as a poultice to an open wound, such as the eye, skin, mucosa, or the wall of an abscess.³⁻⁵

Most infections in humans usually invade the subcutaneous tissue or muscles⁶ but may also occur in the abdominal cavity,⁷ pleura,⁸ genitourinary tract,⁹ eye,¹⁰ spinal canal,¹¹ and brain. Cerebral infection is the most serious complication without characteristic clinical manifestations; it causes headache, seizure, hemiparesis, or other neurologic deficits. It is difficult to make a preoperative diagnosis, and most cerebral sparganoses are diagnosed by surgical resection of the worm and pathologic examination.¹⁻¹⁷ However, with the development of serologic techniques and radiologic instruments, proper diagnosis of cerebral sparganosis could be established before surgery. To date, to our knowledge imaging findings of cerebral sparganosis have been reported sporadically, most of which^{4,5,17,18} were published in the 1990s, but the features on

CT and MR examinations had not previously been described in detail. The purpose of this study was to analyze retrospectively if CT and MR examinations of cerebral sparganosis can be used for correct preoperative diagnosis and to search for new findings.

Materials and Methods

Patients

A total of 25 consecutive patients (13 male, 12 female; age range, 9–83 years) with cerebral sparganosis were analyzed retrospectively between 2000 and 2006. A total of 15 patients underwent MR imaging, 2 patients had CT scans, and the remaining 8 had both CT and MR scans. CT and MR examinations were performed on the same day. All MR scanning was performed before and after intravenous administration of contrast material. However, only 4 patients had contrast-enhanced CT scanning. Our institutional review board approved this study, and informed consent was not required from each patient.

The diagnosis in all patients was based on the combined results of various tests (Table 1): clinical manifestations; history of whether the patient ever ate the raw or uncooked flesh of a frog or a snake, applied them to the open wound, or drank infected water; a positive result of enzyme-linked immunosorbent assay (ELISA) on serum and CSF for sparganosis-specific antibody; and characteristic CT and MR findings.

Imaging Analysis

We performed all MR examinations with a 1.5T superconducting scanner (Gyrosan-Intera; Philips Medical Systems, Best, The Netherlands) with a quadrature head coil for signal intensity collection using the following sequences: axial and sagittal spin-echo T1-weighted (TR, 500 ms; TE, 20 ms), axial and coronal or sagittal turbo

Received February 6, 2007; accepted after revision March 11.

From the Departments of Radiology (T.S., W.-W.M., Z.-Z.L.), Neurology (B.-R.Z.), and Pathology (H.-C.G., F.Z.), The Third Affiliated Hospital of Guangzhou Medical College, Guangdong, China; and the Imaging Center (W.-S.W.), Guangdong 999 Brain Hospital, Guangdong, China.

Please address correspondence to Ting Song, Department of Radiology, The Third Affiliated Hospital of Guangzhou Medical College, No.63 Duobao Rd, Guangzhou, Guangdong, China 510150; email: gzflair@163.com

DOI 10.3174/ajnr.A0659

Table 1: Summary of clinical features, history, methods, and results in 25 patients with cerebral sparganosis

Patient No./ Age (y)/Sex	Imaging Modalities	History	Clinical Manifestations	Results of ELISA		Surgery*
				Serum	CSF	Worm Found
1/80/M	CT‡, MR§	Raw snake ingestion 40 years previously	Headache and seizures for 10 years, left hemiparesis for 2 years	+	+	Degenerated
2/45/F	CT‡, MR§	Uncooked frog ingestion 16 years previously	Headache, seizures, and right hemiparesis for 6 years	+	+	Live
3/53/F	CT‡, MR§	Uncooked frog ingestion 13 years previously	Headache, intermittent seizures, and left hemiparesis for 2 years	+	+	Degenerated
4/24/F	CT‡, MR§	Contaminated water drinking for 6 years	Headache and focal seizures for 7 years	+	+	Degenerated
5/9/M	CT†, MR§	Uncertain	Headache, intermittent seizures for 2 years	+	–	Live
6/14/M	CT†, MR§	Raw snake ingestion 6 years previously	Seizures and left hemiparesis for 4 years	+	+	Live
7/39/M	MR§	Uncertain	Headache and seizures for 5 years	+	+	Degenerated
8/34/M	CT†	Uncertain	Seizures, left hemiparesis for 8 years	+	+	Live
9/37/F	CT†, MR§	Flesh of frog applied to the skin wound 5 years previously	Headache and seizures for 3 years, right hemiparesis for 8 months	+	+	Degenerated
10/28/F	CT†	Flesh of snake applied to skin wound 10 years previously	Focal seizures for 7 years, right hemiparesis for 13 months	+	–	Degenerated
11/36/F	CT†, MR§	Contaminated water drinking for 2 years	Headache for 3 years, right hemiparesis for 1 year	+	+	Live
12/38/M	MR§	Contaminated water drinking 19 years previously	Generalized seizures for 6 years, right hemiparesis for 11 months	+	+	Degenerated
13/47/M	MR§	Flesh of frog applied to abscess on back 13 years previously	Focal seizures for 8 years, right hemiparesis for 1 year	+	+	Degenerated
14/42/M	MR§	Contaminated water drinking 20 years previously	Headache, focal seizures for 3 years	–	+	Degenerated worm found
15/83/F	MR§	Raw frog ingestion 46 years previously	Headache for 30 years, right hemiparesis for 15 months	+	+	Degenerated
16/45/M	MR§	Raw snake ingestion 9 years previously	Generalized seizures for 6 years	–	+	Degenerated
17/41/F	MR§	Raw frog ingestion 17 years previously	Seizures and right hemiparesis for 7 years	+	–	Degenerated
18/43/F	MR§	Raw snake ingestion 14 years previously	Headache, seizures for 9 months	+	+	Degenerated
19/38/M	MR§	Raw frog ingestion 9 years previously	Headache, seizures for 4 years; left hemiparesis for 14 months	+	–	Degenerated
20/29/F	MR§	Frog ingestion for 7 years	Seizures for 3 years	–	+	Degenerated
21/37/M	MR§	Raw snake ingestion 11 years previously	Headache and seizures for 2 years; right hemiparesis for 15 months	+	–	Degenerated
22/48/M	MR§	Uncooked frog ingestion 7 years previously	Headache and seizures for 3 years	+	+	Degenerated
23/26/F	MR§	Uncooked snake ingestion 5 years previously	Headache and seizures for 3 years	+	+	None
24/31/F	MR§	Uncooked snake ingestion 5 years previously	Focal seizures for 2 years	+	+	Degenerated
24/31/F	MR§	Contaminated water drinking 11 years previously	Headache and seizures for 6 years	+	–	Degenerated
25/20/M	MR§	Uncertain	Focal seizures for 9 months	+	+	Degenerated

Note:—ELISA indicates enzyme-linked immunosorbent assay; +, positive; –, negative.

* In this study, craniotomy was performed in 18 patients and a stereotactic targeting biopsy in 7 patients.

† Unenhanced CT scanning.

‡ Unenhanced, contrast-enhanced CT scanning.

§ Unenhanced, contrast-enhanced MR scanning.

spin-echo T2-weighted (TR, 3000 ms; TE, 110 ms), and axial fluid-attenuated inversion recovery (FLAIR; TR, 8000 ms; TE, 120 ms; inversion time, 110 ms) sequence scanning on precontrast MR imaging. After intravenous injection of gadopentetate dimeglumine (Magnevist; Schering, Berlin, Germany) (0.1–0.2 mmol/kg body weight), T1-weighted axial, coronal, and sagittal images were obtained. The section thickness was 8 mm with a gap of 0.8 mm, acquisition matrix of 256 × 256, and a signal intensity acquisition average of 3 to 4 times.

We obtained all CT studies with an Aura spiral scanner (Philips Medical Systems) in 8 patients using the following parameters: section thickness, 8 mm; gap, 8 mm; pitch, 1; tube current, 250 mA; and voltage, 125 kV. Four patients underwent contrast-enhanced CT scanning after intravenous injection of iopromide (Ultravist 300; Schering) (80–100 mL).

Two radiologists retrospectively reviewed the CT and MR images by means of consensus on the number, location, size, shape, and intensity of the lesions; pattern of contrast enhancement; and any other possible new findings. Finally, a craniotomy was performed in 18 patients and a stereotactic targeting biopsy in 7 patients.

Results

The CT and MR images revealed lesions at varying stages. All patients had edema and degeneration of the white matter, which showed hypoattenuation on unenhanced CT images, hypointensity on T1-weighted images, and hyperintensity on T2-weighted images (Figs 1–3). Twenty-two patients demonstrated ipsilateral ventricular dilation (Fig 2), and the remaining 3 showed ipsilateral ventricular compression. MR images

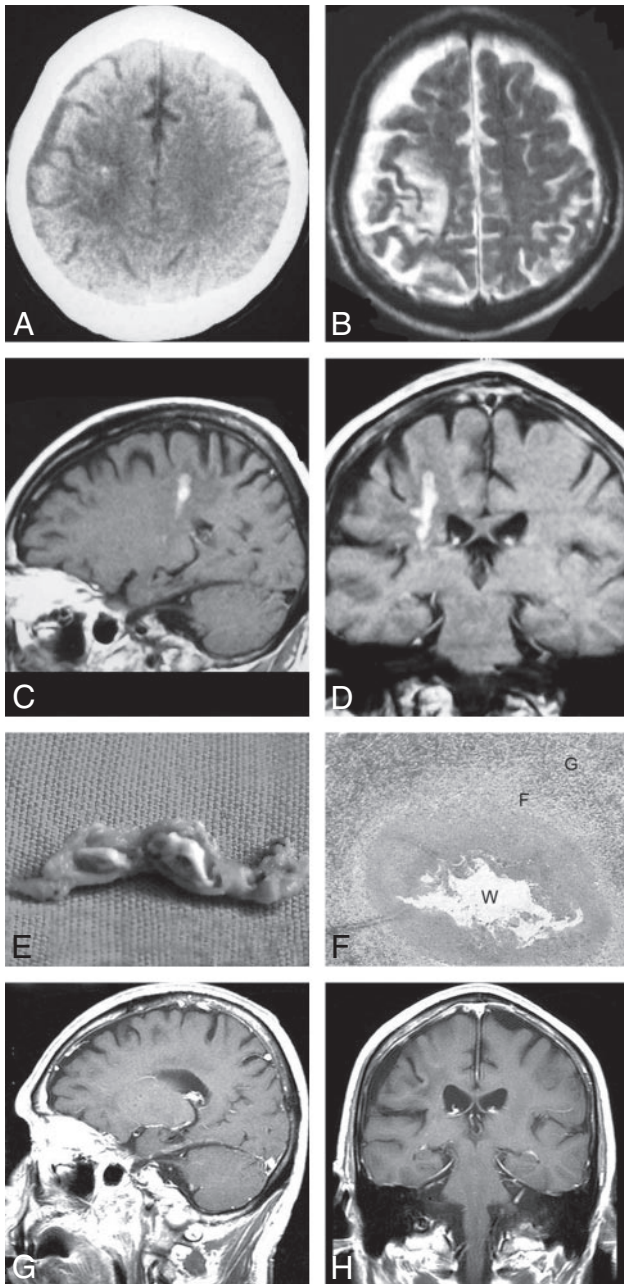


Fig 1. Case 1. Images of the brain of an 80-year-old man with a history of headache, seizure, and left hemiparesis for 2 years. *A*, Precontrast CT scan shows patchy area of hypodensity in the white matter of the right parietal lobe with a punctate calcification located centrally. *B*, Axial T2-weighted MR image of the same day shows hyperintense area and cortical atrophy in the right parietal lobe. However, calcification seen on CT image cannot be found on MR images. *C–D*, Sagittal and coronal postcontrast images show tunnel-shaped enhancement representing inflammatory granuloma. No ipsilateral ventricular dilation is seen. *E*, Postoperative gross photograph of resected specimen shows a degenerated worm of *Spirometra mansoni* surrounded by inflammatory granulomatous tissues. *F*, Photomicrograph of histologic specimen shows a removed degenerated worm (*W*) surrounded by collagen capsule (*C*) and peripheral inflammatory cells and gliosis (*G*) (H&E stain $\times 40$). *G–H*, Sagittal and coronal postcontrast images 1 year after a craniotomy in the same patient show lesions excised, with edematous area in the right parietal lobe.

demonstrated cortical atrophy in 23 patients, and cortical atrophy was seen on CT images in 8 patients. CT images showed small, punctate calcifications in 6 patients (Figs 1–3), but these calcifications were seen on MR imaging in only 3 patients. Calcifications were in or out of the area of the contrast enhancement. The ipsilateral ventricular dilation and calcifica-

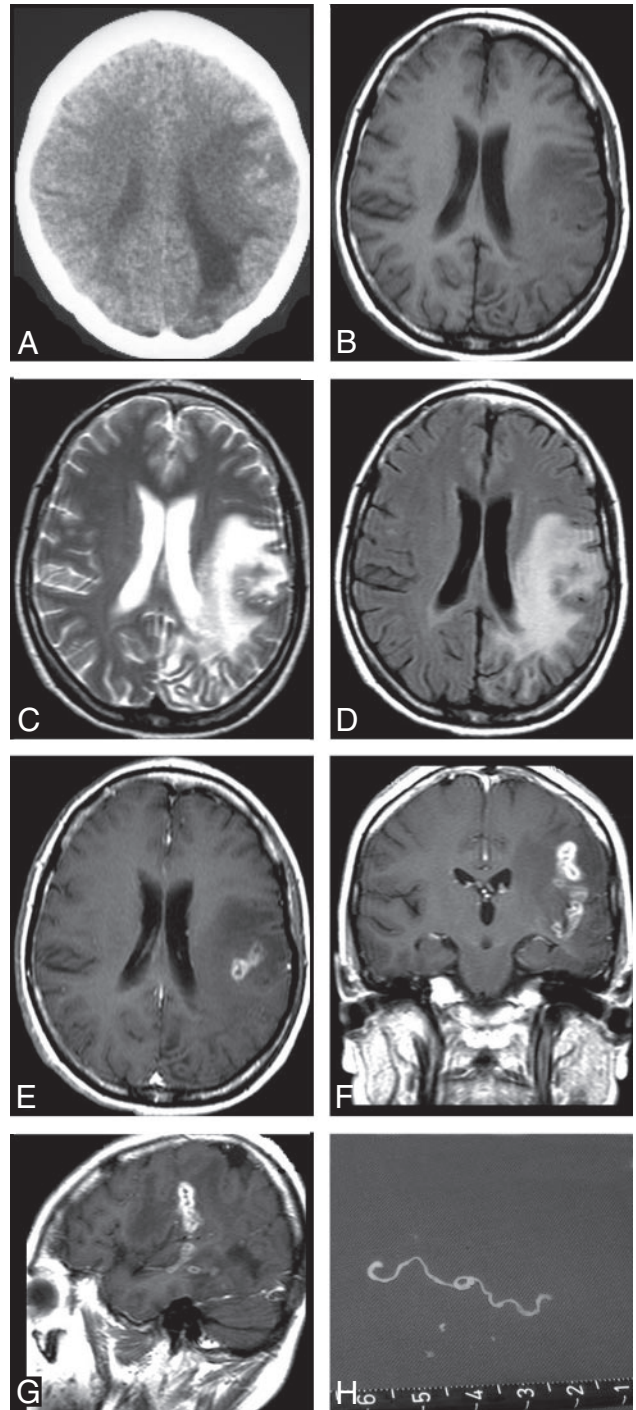


Fig 2. Case 2. Images of the brain of a 45-year-old woman with a 6-year history of severe headache, intermittent seizures, and right hemiparesis. *A*, Precontrast CT scan reveals unilateral extensive area of low attenuation in the white matter of the left parietal lobe, with ipsilateral ventricular dilation. Small, punctate calcifications are seen in the left parietal lobe. *B–D*, Axial T1-weighted (*B*), T2-weighted (*C*), and FLAIR images (*D*) of the same section show a wide area of hypointensity on T1-weighted image (*B*), heterogeneous hyperintensity on T2-weighted (*C*) and FLAIR images (*D*), with a small central area of isointensity or slight hyperintensity on T2-weighted image (*C*), corresponding to isointensity or hypointensity on FLAIR image (*D*), representing encephalomalacia. *E–G*, Postcontrast axial (*E*), coronal (*F*), and sagittal (*G*) T1-weighted images show a tunnel about 5 cm in length and 1.5 cm in width, appearing as a hollow tube located in the left temporal and parietal lobe. *H*, Intraoperative photograph shows a whitish, wrinkled, threadlike live worm approximately 6 cm in length with slow peristalsis.

tions represented old lesions at the late stage. (One of the characteristics of cerebral sparganosis is the presence of new and old lesions alternately.)

Table 2: Common CT and MR characteristics of cerebral sparganosis

Lesion	CT		MR	
	Finding	Number	Finding	Number
White matter degeneration	+	10	+	23
Cortical atrophy	+	8	+	23
Ipsilateral ventricle dilation	+	9	+	20
Ipsilateral ventricle compression	-	0	+	3
Punctate calcification(s)	+	6	+	3
Hemorrhage	+	4	+	4
Tunnel sign*	-	0	+	10
Bead-shaped enhancement†	+	1	+	13
Single-ring enhancement	+	2	-	0
Nodular enhancement	+	1	-	0

Note:—+ indicates positive; -, negative.

* Tunnel sign is commonly seen on coronal and sagittal postcontrast MR images. The tunnel is about 4 cm in length (range, 2–6 cm) and 0.8 cm in width (range, 0.5–1.5 cm) and shows hypointensity on T1-weighted images, hyperintensity on T1-weighted images, and marked enhancement on postcontrast MR images.

† Bead-shaped enhancement is aggregated ringlike enhancement, usually 3 to 6 rings, with a smooth margin; ring wall thickness is 0.1 to 0.2 cm.

The most important, and also characteristic, finding was the tunnel sign (Table 2) on the postcontrast MR images ($n = 10$). The tunnel sign appeared hypointense on T1-weighted images and slightly hyperintense or isointense on T2-weighted images. There was obvious enhancement on the postcontrast MR images, particularly on coronal and sagittal postcontrast MR images (Figs 1C, D and 2C, D). The tunnel was about 4 cm in length (range, 2–6 cm) and 0.8 cm in width (range, 0.5–1.5 cm) and was column or fusiform shaped. On postcontrast MR images, the tunnel represented the moving track of a migrating worm, appearing as a solid or hollow tube, which corresponded to inflammatory granulomas according to the postoperative pathologic examination. No tunnel sign could be seen on CT images, possibly because of the lack of multiplanar scanning.

The second most common feature was a conglomerated ringlike enhancement (Table 2), which was seen as bead shaped, usually 3 to 6 rings, on MR images ($n = 13$, Fig 3C, D), but a solitary ring-shaped enhancement on CT images was common ($n = 2$). The wall of the ring was smooth, with isoattenuation on nonenhanced CT images, hypointensity on T1-weighted images, isointensity or slight hyperintensity on T2-weighted images, and marked enhancement on postcontrast CT and MR images. The internal components of the rings appeared slightly hyperattenuated on unenhanced CT images, hypointense on T1-weighted images, hyperintense on T2-weighted images, and showed no enhancement on postcontrast CT and MR images. Each ring was approximately 0.6 cm in diameter (range, 0.2–0.8 cm), and the wall of the ring was between 0.1 cm and 0.2 cm in diameter.

However, nodular or solitary ring enhancement, rather than the tunnel sign and aggregated ring-shaped enhancement, was common on the postcontrast CT images. Confirmed by postoperative specimens and pathologic examinations, cerebral hemorrhage was seen in 4 patients and appeared slightly hyperintense on T1-weighted images and intermediately intense on T2-weighted images. These findings corresponded to high attenuation on CT plain scanning images.

All but 1 patient had a unilateral lesion (right hemisphere in 13 patients and left hemisphere in 11). In 16 patients, the

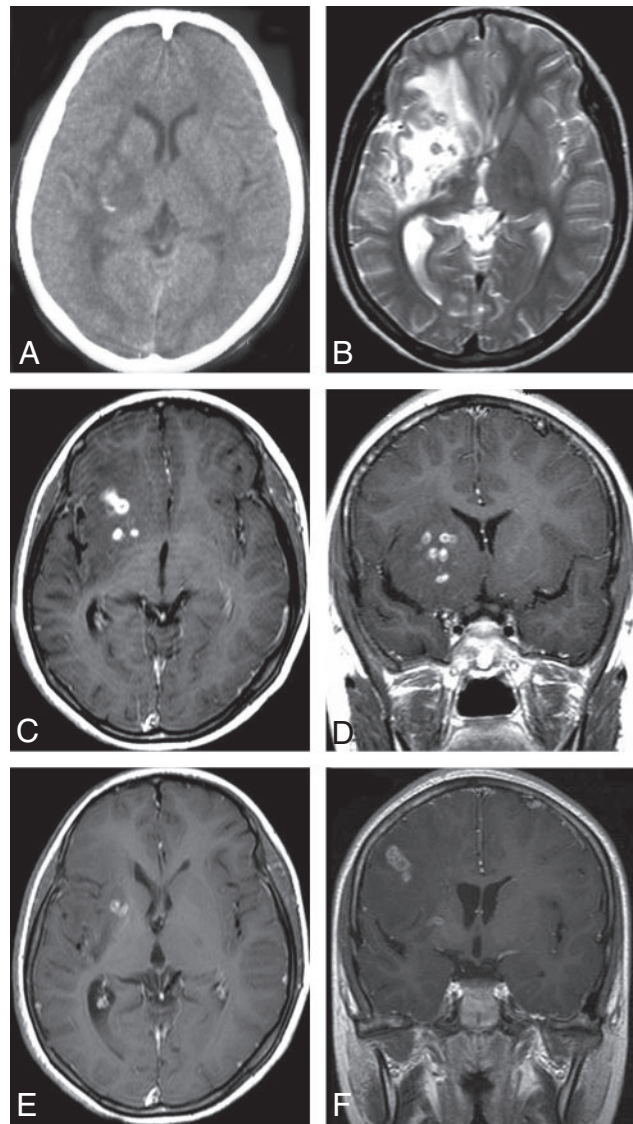


Fig 3. Case 6. Images of the brain of a 14-year-old boy with a 4-year history of seizures and left hemiparesis. *A*, Precontrast CT scan shows an extensive area of low attenuation in the right basal ganglia with a punctate calcification centrally. *B*, Axial T2-weighted image of the same section as the CT image in (*A*) shows hyperintense area in the right basal ganglia. However, calcification seen on CT image cannot be shown clearly on MR image. *C–D*, Postcontrast axial (*C*) and coronal (*D*) T1-weighted images show bead-shaped enhancement in the right basal ganglia. *E–F*, After 4 months, postcontrast axial (*E*) and coronal (*F*) T1-weighted images of the same patient show the tunnel-shaped enhancement in the right parietal lobe with small amounts of residual bead-shaped enhancement in the right basal ganglia, representing the migration of the worm and lesions shifting from the right basal ganglia to the right parietal lobe. Preoperative ELISA on serum and on CSF revealed strongly positive against *Spirometra mansoni*. A live worm was found at craniotomy.

lesions were located in the posterior part of the cerebral hemisphere (occipital, posterior temporal, and posterior parietal lobes). In the remaining 9 patients, the lesions were located in the anterior part of the cerebral hemisphere (frontal, anterior temporal, and anterior parietal lobes). In 10 patients, the lesions were solitary. In another 15 patients, there was multifocality and the lesions extensively involved the white matter of the parietal, frontal, or occipital lobes, or the basal ganglia (Fig 3). Only 1 case of multiple lesions involving the white matter of the bilateral parietal and occipital lobes was seen on MR images.

A craniotomy was performed in 18 patients and a stereotactic targeting biopsy in 7 patients. In 5 patients, an intact live, whitish, stringlike worm was found, showing slow peristalsis (Fig 2H). The mean length of these live worms was 11 cm (range, 5–18 cm). Microscopic examination revealed dead or disintegrated worms in 20 patients; these worms were segmented, compact, eosinophilic structures (Fig 1E). The inflammatory granuloma and reactive exudate including gliosis, histiocytes, eosinocytes, and lymphocytes surrounded the tegument of the degenerated worm (Fig 1F). Histologic examination revealed all resected specimens to be cerebral sparganosis. ELISA on serum and on CSF was positive for *Spirometra mansoni* in 22 patients and 19 patients, respectively (Table 1). Seventeen patients were definitely diagnosed preoperatively on the basis of imaging features, clinical history, and ELISA.

Discussion

Although sparganosis has been reported worldwide, most cases occur in Southeast Asia, China, Japan, and Korea, and less commonly in the United States and Europe.¹⁶ The common routes of infection in humans were described above, but the exact route of infection to the brain is still uncertain. The larvae may migrate through the loose connective tissues of the foramina of the skull base around the nerves or vessels.¹⁹

In our study, 12 patients (48%) had a history of eating raw or uncooked frog or snake that was infected with sparganum. They lived in rural areas where the raw flesh of frogs, snakes, or chickens were considered tonic. Five patients (20%) had applied animal's flesh (possibly infected host) as a poultice to an open wound because it was taken as a folk remedy for treatment of the wound. Four patients had a history of drinking contaminated water. The remaining 4 patients had no certain history of being infected. Therefore, we believe that health education concerning sparganosis and sanitary dietary habits should be recommended in rural areas.

The course of the disease in our study was long, varying from 8 months to 30 years because of the slow growth of the sparganum. The most common symptoms were headache, seizure, and hemiparesis. Because all the symptoms were nonspecific, it was very difficult to make a preoperative diagnosis. Imaging examinations, especially MR imaging, played an important role in the diagnosis and differential diagnosis of cerebral sparganosis.

Chang et al^{4,20} described the CT features as white matter hypoattenuation with adjacent ventricular dilation; irregular or nodular enhancing lesions; and small, punctate calcifications. However, in our study we found that MR scanning (in particular, contrast-enhanced MR scanning) proved to be superior to CT in the demonstration of the extent, number, and shape of the lesions.

Most of the lesions were multifocal and were located in the white matter of the parietal, occipital, temporal, or frontal lobe. The less common sites were the basal ganglia, insula, and cerebella.¹⁹ The primary characteristic of cerebral sparganosis is that the live worm migrates with undulating motion. The migrating worm makes a tunnel along the track of motion. A tunnel sign was conspicuously seen on postcontrast sagittal and coronal MR images as fusiform shaped, appearing hypointense on T1-weighted images, slightly hyperintense or isointense on T2-weighted images, and column or fusiform

shaped on postcontrast MR images. However, a solitary ring or nodular enhancement was more common on CT images, which may have been relative to the scarcity of coronal and sagittal scanning on CT images. On the other hand, the cause may have been the result of fewer patients undergoing contrast enhancement CT scanning in our study. As far as we know, this sign has not been reported in the CT and MR literature but is a distinctive feature. The column-shaped or fusiform-shaped tunnel showed a solid or hollow appearance with a smooth, well-defined margin. From a pathologic standpoint, the enhancing tunnels were the reactive inflammatory tissue or granuloma enwrapping the worm.

The second characteristic of cerebral sparganosis is the conglomerated ring or bead-shaped enhancement, which represents an inflammatory granuloma. The wall of the ring-shaped granulomas is hypointense on T1-weighted images and isointense or slightly hypointense on T2-weighted images. The cause of the hypointensity or isointensity of the wall of the ring on T2-weighted images may be the same as those of a pyogenic abscess that presumably resulted from the free radicals produced by macrophages.²¹

The third characteristic of cerebral sparganosis is the alternate change of varying stages in the same image because of the long course of the disease, from the initial attack to admission to the hospital. Small, punctate calcifications were around or in the degenerated or dead worm produced by deposition of calcareous corpuscles (particles containing calcifications). The calcifications could be clearly revealed on CT images but were obscure on MR images because of the insensitivity to calcifications. Meanwhile, unilateral ventricular dilation and focal cerebral cortical atrophy hinting the chronic stage may be caused by long-standing injuries by the worm. Cortical atrophy and bead-shaped enhancement denoting the chronic and acute phases, respectively, usually coexisted in the same lesion. White matter edema may be caused by a capillary or venous injury produced by the migrating worm, which corresponds to hypointensity on T1-weighted images, hyperintensity on T2-weighted images, and hypoattenuation on CT images. However, these changes were not characteristic of the final diagnosis. There was a sharp contrast with previous related reports.^{20,22} Focal hemorrhage was rarely seen on CT and MR images, though hemorrhage was confirmed intraoperatively and postoperatively.

Compared with other studies reported in the literature,^{4,5,12,19} the tunnel sign in our study was our first concern because it represented the migration of the worm. Although other imaging findings, such as the bead-shaped enhancement and white matter degeneration, were also reported, our study integrated imaging data, clinical history, and ELISA. Moreover, all the lesions in our study were confirmed by surgical resection and pathologic examination.

The differential diagnosis of cerebral sparganosis includes brain tumors and other inflammatory granulomas.^{19,20} In particular, metastatic brain tumors mimic cerebral sparganosis on CT and MR imaging, but metastatic tumors often have a mass effect to compress the ventricle, and sparganosis has adjacent ventricular dilation. On postcontrast MR images, sparganosis showed the tunnel sign, but metastatic tumors and other inflammatory granulomas did not. The small, punctate calcifications may be helpful in the diagnosis but cannot be

shown clearly on MR imaging. If the mass effect occurred, it was hard to distinguish cerebral sparganosis from a brain tumor unless clinical data and ELISA were used. If cortical atrophy and degeneration of white matter existed, sparganosis should be distinguished from chronic cerebral ischemia, which was predominately common in one of our patients (an 80-year-old man) without a tunnel sign or bead-shaped enhancement on MR images.

Besides the imaging appearances and a dependable history, ELISA has been very useful in the correct diagnosis of cerebral sparganosis.^{19,23} The live worm was approximately 5 to 18 cm long, whitish, and thread shaped, with serpiginous peristalsis. The degenerated worm in the brain was usually surrounded by collagen fibers, inflammatory cells, and gliosis.

In conclusion, cerebral sparganosis exhibited certain features on the CT and MR images. The most characteristic finding was the tunnel sign on postcontrast coronal and sagittal MR images, and the most common finding was multiple conglomerated ring-shaped (bead-shaped) enhancements. MR, especially contrast enhancement MR imaging, is superior to CT in the demonstration of the extent, number, and internal structure of the lesions except with small, punctate calcifications. Other important findings included cortical atrophy, white matter degeneration, and ipsilateral ventricular dilation of the lesions produced by a migrating worm. Combined with clinical history and ELISA, a correct preoperative diagnosis of cerebral sparganosis could be established.

References

- Mueller JF. The biology of *Spirometra*. *J Parasitol* 1974;60:3–14
- Muller JF, Hart EP, Walsh WP. Human sparganosis in the United States. *J Parasitol* 1963;49:294–96
- Dunn IJ, Palmer PE. Sparganosis. *Semin Roentgenol* 1998;33:86–88
- Chang KH, Cho SY, Chi JG, et al. Cerebral sparganosis: CT characteristics. *Radiology* 1987;165:505–10
- Fan KJ, Pezeshkpour GH. Cerebral sparganosis. *Neurology* 1986;36:1249–51
- Cho JH, Lee KB, Yong TS, et al. Subcutaneous and musculoskeletal sparganosis: imaging characteristics and pathologic correlation. *Skeletal Radiol* 2000;29:402–08
- Lee JH, Yu JS, Park MS, et al. Abdominal sparganosis presenting as an abscess with fistulous communication to the bowel. *AJR Am J Roentgenol* 2005;185:1084–85
- Tanaka S, Maruyama H, Ishiwata K, et al. A case report of pleural sparganosis. *Parasitol Int* 1997;46:73–75
- Jeong HJ. Fournier's gangrene associated with sparganosis in the scrotum. *Urology* 2004;63:176–77
- Yoon KC, Seo MS, Park SW, et al. Eyelid sparganosis. *Am J Ophthalmol* 2004;138:873–75
- Kudesia S, Indira DB, Sarala D, et al. Sparganosis of brain and spinal cord: unusual tapeworm infestation (report of two cases). *Clin Neurol Neurosurg* 1998;100:148–52
- Kim DG, Paek SH, Chang KH, et al. Cerebral sparganosis: clinical manifestations, treatment, and outcome. *J Neurosurg* 1996;85:1066–71
- Kim J, Park JH, Ryu YH, et al. Tc-99m ECD SPECT and FDG PET in partial status epilepticus resulting from cerebral sparganosis. *Clin Nucl Med* 2006;31:307–09
- Nobayashi M, Hirabayashi H, Sakaki T, et al. Surgical removal of a live worm by stereotactic targeting in cerebral sparganosis. Case report. *Neurol Med Chir (Tokyo)* 2006;46:164–67
- Sundaram C, Prasad VS, Reddy JJ. Cerebral sparganosis. *J Assoc Physicians India* 2003;51:1107–09
- Cummings TJ, Madden JF, Gray L, et al. Parasitic lesion of the insula suggesting cerebral sparganosis: case report. *Neuroradiology* 2000;42:206–08
- Jeong SC, Bae JC, Hwang SH, et al. Cerebral sparganosis with intracerebral hemorrhage: a case report. *Neurology* 1998;50:503–06
- Kradel J, Drolshagen LF, MacDade A. MR and CT findings in cerebral sparganosis. *J Comput Assist Tomogr* 1993;17:989–90
- Moon WK, Chang KH, Cho SY, et al. Cerebral sparganosis: MR imaging versus CT features. *Radiology* 1993;188:751–57
- Chang KH, Chi JG, Cho SY, et al. Cerebral sparganosis: analysis of 34 cases with emphasis on CT features. *Neuroradiology* 1992;34:1–8
- Haimes AB, Zimmerman RD, Morgello S, et al. MR imaging of brain abscesses. *AJR Am J Roentgenol* 1989;152:1073–85
- Anegawa S, Hayashi T, Ozuru K, et al. Sparganosis of the brain. Case report. *J Neurosurg* 1989;71:287–89
- Okamura T, Yamamoto M, Ohta K, et al. Cerebral sparganosis mansoni—case report. *Neurol Med Chir (Tokyo)* 1995;35:909–13